Reference: *Biol. Bull.* **188**: 136–145. (April, 1995)

Microtubule Arrays During Ooplasmic Segregation in the Medaka Fish Egg (*Oryzias latipes*)

V. C. ABRAHAM[1], A. L. MILLER[2], AND R. A. FLUCK[1],*

[1]*Biology Department, Franklin and Marshall College, Lancaster, Pennsylvania 17604-3003; and*
[2]*Marine Biological Laboratory, Woods Hole, Massachusetts 02543*

Abstract. We used indirect immunofluorescence to study microtubule arrays in the medaka egg between fertilization (normalized time, $T_n = 0$) and the first cleavage ($T_n = 1.0$). Eggs were fixed at various times after fertilization and examined with conventional fluorescence microscopy, laser scanning confocal microscopy, and three-dimensional fluorescence microscopy. Soon after the eggs were fertilized ($T_n = 0.02$), we saw microtubules oriented perpendicular to the plane of the plasma membrane but none parallel to the plasma membrane. Later ($T_n = 0.08$), we saw an array of microtubules oriented more or less parallel to the plasma membrane but having no apparent preferred orientation with respect to the animal-vegetal axis of the egg. In the interpolar regions of the egg, this network increased in density by $T_n = 0.24$ and remained a constant feature of the ooplasm until the first cleavage. From $T_n = 0.30$ to 0.76 the polar regions of the egg contained dense arrays of organized microtubules. At the animal pole, microtubules radiated from a site near the pronuclei; while at the vegetal pole, an array of parallel microtubules was present. Injection of the weak ($K_D = 1.5\ \mu M$) calcium buffer 5,5′-dibromo-BAPTA disrupted the radial pattern of microtubules near the animal pole but had no apparent effect on the parallel array of microtubules near the vegetal pole. Because this buffer has previously been shown to suppress a zone of elevated cytosolic calcium at the animal pole and to disrupt ooplasmic segregation in this egg, the results of the present study (1) are consistent with a model in which microtubules are required for ooplasmic segregation in the medaka egg, and (2) suggest that the normal function of a microtubule-organizing center at the animal pole of the egg requires a zone of elevated calcium.

Received 20 June 1994; accepted 11 January 1995.

* To whom correspondence should be addressed.

Introduction

Ooplasmic segregation in the medaka egg consists of the approximately simultaneous streaming of ooplasm toward the animal pole, the saltatory movement of parcels toward the animal pole and vegetal pole, and the movement of oil droplets toward the vegetal pole (Abraham *et al.*, 1993a; Webb and Fluck, 1993). These movements are roughly simultaneous and are essentially completed during the first cell cycle. Streaming of ooplasm toward the animal pole is inhibited by cytochalasin D and thus presumably requires microfilaments (Webb and Fluck, 1993), whereas saltatory movements and the movement of oil droplets toward the vegetal pole are both inhibited by microtubule poisons and thus presumably require microtubules (Abraham *et al.*, 1993a). All of these movements can be easily observed in the optically clear medaka egg, in which a thin ($\approx 15\ \mu m$ thick) peripheral layer of ooplasm surrounds a large, central yolk vacuole.

In a number of diverse animals, including annelids (Astrow *et al.*, 1989), ctenophores (Houliston *et al.*, 1993), echinoderms (Harris *et al.*, 1980), ascidians (Sawada and Schatten, 1988), and amphibians (Elinson and Rowning, 1988; Houliston and Elinson, 1991; Schroeder and Gard, 1992; Elinson and Palaček, 1993), a network of microtubules that forms during the first cell cycle is required for the movement of specific components of the ooplasm, including the pronuclei. In the present study, we describe the development of such an array of microtubules during the first cell cycle of the medaka egg. Previous studies of microtubules in teleost embryos either have provided very little information (Beams *et al.*, 1985) or have been done on later stages of development (Strähle and Jesuthasan, 1993; Solnica-Krezel and Driever, 1994).

We also pursued the hypothesis that gradients of cytosolic free Ca^{2+} organize the multimolecular assemblies

involved in ooplasmic segregation in the medaka egg. Zones of elevated calcium are present at the animal and vegetal poles of the medaka egg during segregation (Fluck *et al.*, 1992). Moreover, injection of 5,5′-dibromo-BAPTA (hereafter referred to as dibromo-BAPTA), a weak calcium buffer that dissipates cytosolic calcium gradients (Pethig *et al.*, 1989; Speksnijder *et al.*, 1989; Fluck *et al.*, 1992), inhibits ooplasmic segregation in this egg (Fluck *et al.*, 1994). In the present study we monitored the effects of this buffer on the spatiotemporal pattern of microtubules and on pronuclear movements. A preliminary account of these findings has been published (Abraham *et al.*, 1993b).

Materials and Methods

Procedures

Methods for removing gonads from breeding medaka and for the *in vitro* fertilization of eggs have been described previously (Abraham *et al.*, 1993a). Some eggs were incubated in 100 μM colchicine (dissolved in buffered saline solution: 111 mM NaCl; 5.37 mM KCl; 1.0 mM $CaCl_2$; 0.6 mM $MgSO_4$; 5 mM HEPES, pH 7.3) for 1 h at room temperature (20°–25°C) before they were fertilized.

Using a high-pressure microinjection system, we injected enough 50 mM dibromo-BAPTA (tetrapotassium salt; containing 5 mM HEPES, pH 7.2, and sufficient $CaCl_2$ to set $[Ca^{2+}]_{free}$ at 100 nM) to raise the cytosolic concentration to 2.7 mM (Fluck *et al.*, 1992). Injections were made within 10° are toward the vegetal pole from the equator within 6 min after fertilization. Control eggs received a comparable volume (*ca.* 1.5 nl) of 150 mM KCl, 5 mM HEPES, pH 7.2.

The procedures for indirect immunofluorescence were those developed by Gard (1991) for the study of microtubules in *Xenopus laevis* eggs. At regular intervals after fertilization, eggs were transferred to fixative solution at room temperature (3.7% formaldehyde, 0.25% glutaraldehyde, 0.2% Triton X-100, 5 mM EGTA, 1 mM $MgCl_2$, 80 mM potassium PIPES, pH 6.8). After 4 h, the eggs were dechorionated with fine forceps and post-fixed in absolute methanol (−20°C) overnight. The eggs were then washed with phosphate-buffered saline (PBS: 128 mM NaCl; 2 mM KCl; 8 mM NaH_2PO_4; 2 mM KH_2PO_4, pH 7.2) and incubated in 100 mM sodium borohydride (in PBS) for 6 h. The eggs were then washed with cold Tris-buffered saline (TBS: 155 mM NaCl; 10 mM Tris-Cl, pH 7.4; 0.1% Nonidet P-40); transferred to Lab-Tek chamber slides (Thomas Scientific, Swedesboro, New Jersey); incubated with a monoclonal mouse anti-α-tubulin antibody (ICN, DM1A; diluted 1:250 with TBS containing 2% bovine serum albumin); washed with TBS for 24 h; incubated with the secondary antibody (rhodamine-conjugated goat anti-mouse IgG, diluted 1:25 with TBS containing 2% bovine serum albumin); and washed for 24 h with TBS. We performed two kinds of antibody controls: omission of the primary antibody and omission of both the primary and the secondary antibodies. To stain the nuclei, we incubated the eggs for 30 min in a solution of Hoechst 33258 (10 $\mu g\ ml^{-1}$) in TBS.

The eggs were mounted between a coverglass and a microscope slide as described previously (Abraham *et al.*, 1993a) and examined by one of three methods. Conventional epifluorescence microscopy was performed with a Nikon Optiphot microscope coupled to a Dage-MTI SIT camera and video monitor; in later replicates, the SIT camera was coupled to a Dage-MTI DSP-2000 image processor. In either case, the image on the monitor was photographed through a Ronchi grating (Rolyn Optics Co., Covina, California; Inoué, 1981). Some eggs were examined with a laser scanning confocal microscope (Zeiss LSCM 410) at the Marine Biological Laboratory.

We also acquired and processed images at the Science and Technology Center at Carnegie-Mellon University. Images at each focal plane were acquired on a multimode microscope (Biological Detection Systems, Inc., Pittsburgh, Pennsylvania) equipped with a 576 × 384 Thompson chip, cooled CCD camera (Photometrics Ltd., Tucson, Arizona). Three-dimensional fluorescence microscopy used the nearest neighbor algorithm to correct for out-of-focus fluorescence (Biological Detection Systems, Inc.) The final three-dimensional representation was generated with the program ANALYZE (Biomedical Imaging Resource, Mayo Foundation, Rochester, Minnesota) on the SGI, Inc., ONYX workstation.

The results summarized herein represent 11 replicate experiments in which we fixed eggs at various intervals after fertilization and three replicate experiments in which we examined the effects of dibromo-BAPTA on microtubules. In all, we have examined a total of 117 eggs from 17 females, including 20 eggs into which we injected dibromo-BAPTA and 8 eggs into which we injected KCl.

Chemicals

Formaldehyde and glutaraldehyde were obtained from Electron Microscopy Sciences (Fort Washington, Pennsylvania); Triton X-100, Nonidet P-40, sodium borohydride, bovine serum albumin, Hoechst 33258, and colchicine from Sigma (St. Louis, Missouri); 5,5′-dibromo-BAPTA from Molecular Probes (Eugene, Oregon); anti-α-tubulin antibody from ICN (Costa Mesa, California); and rhodamine-conjugated goat anti-mouse IgG from Organon Teknika (Malvern, Pennsylvania).

Results

The various events that constitute ooplasmic segregation in the fertilized medaka egg have already been described in detail (Abraham *et al.*, 1993a) and are only

summarized below. To indicate the relative temporal position of these events, we have used a normalized time (T_n) scale in which the time between fertilization and the beginning of cytokinesis is 1 unit. In the range of room temperatures in which the experiments were done (20°–25°C), 1 unit of normalized time corresponds to 75–110 min. Fertilization in the medaka egg is followed by a cortical granule reaction and a contraction, during which the ooplasm and its contents appear to be pulled toward the animal pole. The second meiotic division is completed by $T_n \approx 0.12$ and is followed closely by a second animal-pole-directed contraction at $T_n \approx 0.15$. This second contraction heralds the beginning of ooplasmic segregation in the form of streaming of ooplasm toward the animal pole, saltatory movements of parcels toward both polar regions, and movement of oil droplets (a class of ooplasmic inclusions) of various sizes toward the vegetal pole. At $T_n = 1.0$, the blastodisc divides into two blastomeres. By this time the oil droplets have formed a crude ring around the vegetal pole.

Microtubule network dynamics during ooplasmic segregation

We identified three regions of the medaka egg on the basis of the spatiotemporal pattern of microtubules in them (Figs. 1–3): (1) a region within 30° (≈300 μm) arc of the animal pole; (2) a region within 60° (≈600 μm) arc on both sides of the equator; and (3) a region within 30° (≈300 μm) arc of the vegetal pole. In all regions of the egg except the animal pole, all the microtubules were within 2–3 μm of the surface of the egg and were visible in a single optical section.

$T_n \approx$ *0.02, 0.08, and 0.16.* The earliest time at which we fixed eggs was $T_n = 0.02$; that is, immediately after the contraction that follows the cortical granule reaction. Though we searched the ooplasm everywhere on these eggs (and all of the ooplasm is peripheral, see Introduction), we saw no microtubules parallel to the surface of the egg but saw instead a punctate pattern of fluorescence (Fig. 1A). Analysis of these eggs by three-dimensional fluorescence microscopy suggests that the sources of fluorescence were microtubules oriented perpendicular to the surface of the egg (Fig. 1B). This punctate pattern was a prominent feature of eggs fixed at $T_n = 0.02$ and 0.08 and was less prominent at later stages.

In eggs fixed at $T_n \approx 0.08$, we saw a very sparse network of microtubules oriented parallel to the surface of the egg but having no apparent preferred orientation with respect to the animal-vegetal axis of the egg. This network was roughly confined to the animal hemisphere, and we saw no microtubules in most of the vegetal hemisphere (Fig. 1C, D).

In eggs fixed at $T_n \approx 0.16$—by which time ooplasmic segregation has begun in the form of streaming, saltatory movements, and oil droplet movement—a network of microtubules was present throughout the ooplasm, and the network in the equatorial region was denser than at $T_n \approx 0.08$ (Fig. 1E). The network did not yet appear to have a preferred orientation.

To test for autofluorescence, we examined fixed eggs that were incubated with no antibodies and that were processed for viewing up to the first wash with TBS. We saw no fluorescence at all in these eggs (data not shown). We also examined eggs that were incubated with the secondary antibody but not with the primary antibody. In these eggs, we saw diffuse fluorescence but no linear elements or punctate sources of fluorescence (Fig. 1F). In eggs incubated with 100 μ*M* colchicine before fixation and incubated with both the primary and secondary antibodies, we saw diffuse fluorescence but no microtubules or any punctate sources of fluorescence (data not shown).

The pattern of microtubules in eggs fixed at $T_n \approx 0.16$ is summarized in Fig. 3A.

$T_n =$ *0.24, 0.3, 0.4, 0.76.* In ooplasm near the equator, the network of microtubules was denser than at $T_n = 0.16$ (Fig. 2A; compare with Fig. 1E) but still showed no preferred orientation with respect to the animal-vegetal axis. In contrast, oriented microtubule networks were present near the vegetal pole and animal pole by $T_n = 0.24$ and $T_n = 0.3$, respectively. Near the vegetal pole, an array of (mostly) parallel microtubules was present (Fig. 2B). This "vegetal mat" extended about 30° arc (300 μm) in all directions from the vegetal pole and covered at least 30% of the area of the vegetal hemisphere. The orientation of microtubules was uniform throughout the vegetal mat. Beyond the edges of the mat, the network of microtubules abruptly lost its orientation and became the network characteristic of interpolar ooplasm. Using the z-sectioning function of the LSCM 410, we determined that the thickness of the microtubule network in the vegetal mat (≈2.7 μm) was the same as the thickness of the unoriented microtubule network just outside the mat. The two networks appeared to be continuous with each other and were in the same optical section, suggesting that the two networks are located at the same depth in the ooplasm.

Near the animal pole, microtubules were oriented more or less along meridian lines and appeared to radiate from a microtubule-organizing center near the male and female pronuclei, which were 38.6 ± 6.7 μm ($\bar{X} \pm$ SD, $n = 5$) below the surface of the blastodisc at $T_n \approx 0.76$ (Fig. 2D–I). This network of oriented microtubules extended approximately 30° arc (300 μm) in all directions from the animal pole.

The pattern of microtubule distribution in eggs fixed at $T_n = 0.30$–0.76 is summarized in Fig. 3B.

$T_n =$ *1.0.* In these eggs, the blastodisc has begun to divide into two blastomeres, and essentially all oil droplets have aggregated in a crude ring near the vegetal pole. Each

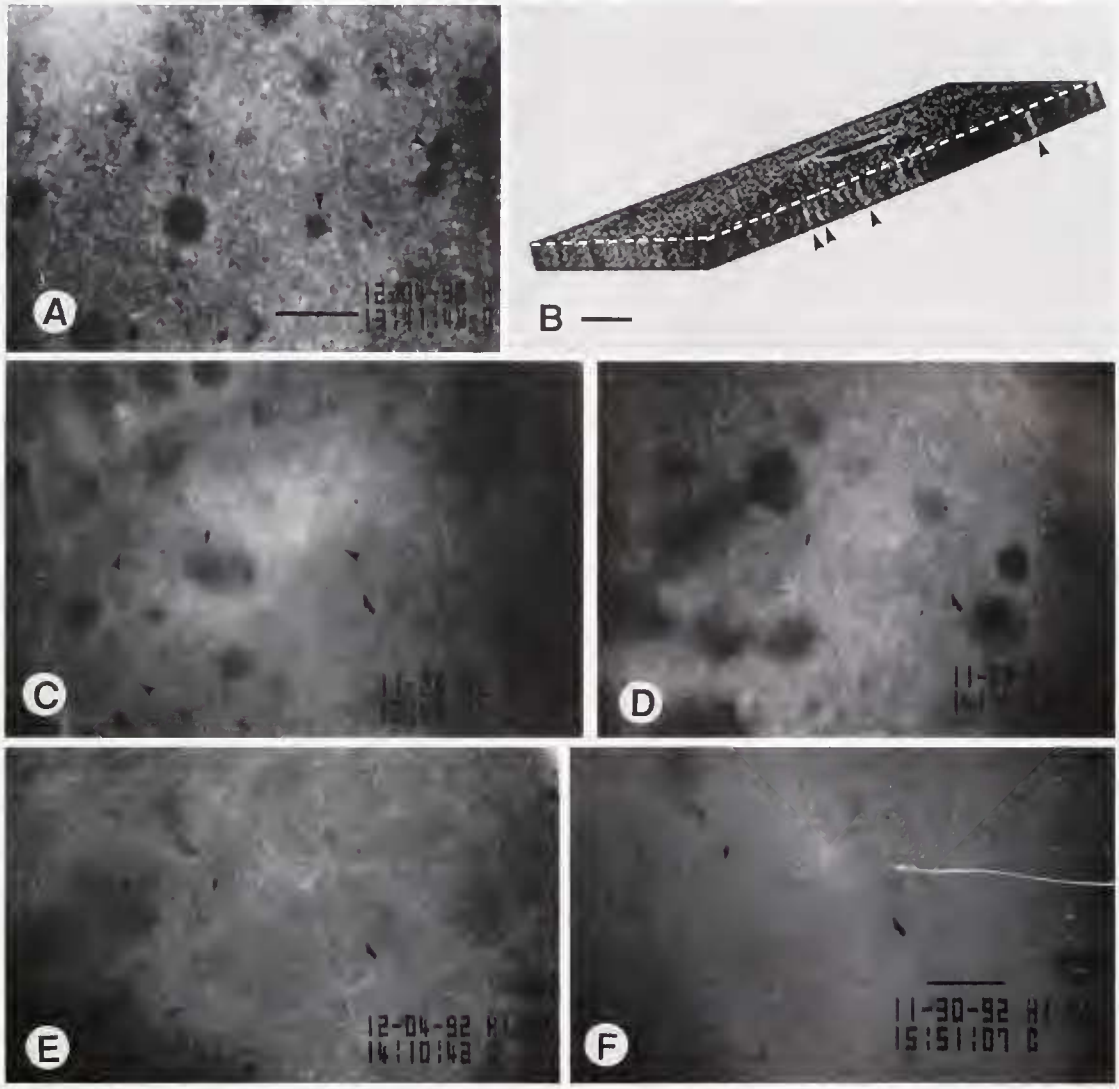

Figure 1. Formation of a network of microtubules in the fertilized egg. A, C, D, E, and F were obtained by conventional epifluorescence microscopy and B by three-dimensional fluorescence microscopy. Scale bars, 10 μm. A, C, D, and E are printed at the same magnification, B at another, and F at another. (A) Ooplasm near the equator of an egg fixed at T_n = 0.02. Characteristic of this stage of development are a punctate pattern of fluorescence throughout the ooplasm and the absence of unambiguous microtubular elements oriented parallel to the plasma membrane. The dark structures (arrowheads) are ooplasmic inclusions. (B) Three-dimensional rendering of optical sections of ooplasm near the equator at T_n = 0.024. Using a 100× objective lens, we made 33 optical sections at steps of 0.158 μm, beginning at the surface of the egg. Visible in this reconstruction are both the punctate pattern at the surface of the egg (the top of the image) and linear elements that are oriented perpendicular to the surface of the egg (arrowheads). Two edges of the reconstruction are marked by a white dashed line. (C) Ooplasm near the animal pole of an egg fixed at T_n = 0.08. Note the presence of unambiguous microtubules in the field (arrowheads). (D) Ooplasm near the vegetal pole of an egg fixed at T_n = 0.08. This image was obtained from the same egg as Fig. 2C. No unambiguous microtubules oriented parallel to the plasma membrane can be seen. (E) Ooplasm near the equator of an egg fixed at T_n = 0.16. The animal-vegetal axis runs from lower left to upper right. This unoriented network is denser than that found at the equator of an egg fixed at T_n = 0.08 (not shown). (F) In eggs not incubated with the primary antibody after fixation (T_n = 0.4), we saw only weak and diffuse fluorescence but saw neither any filamentous structures nor a punctate pattern of fluorescence. These images were obtained by standard epifluorescence microscopy.

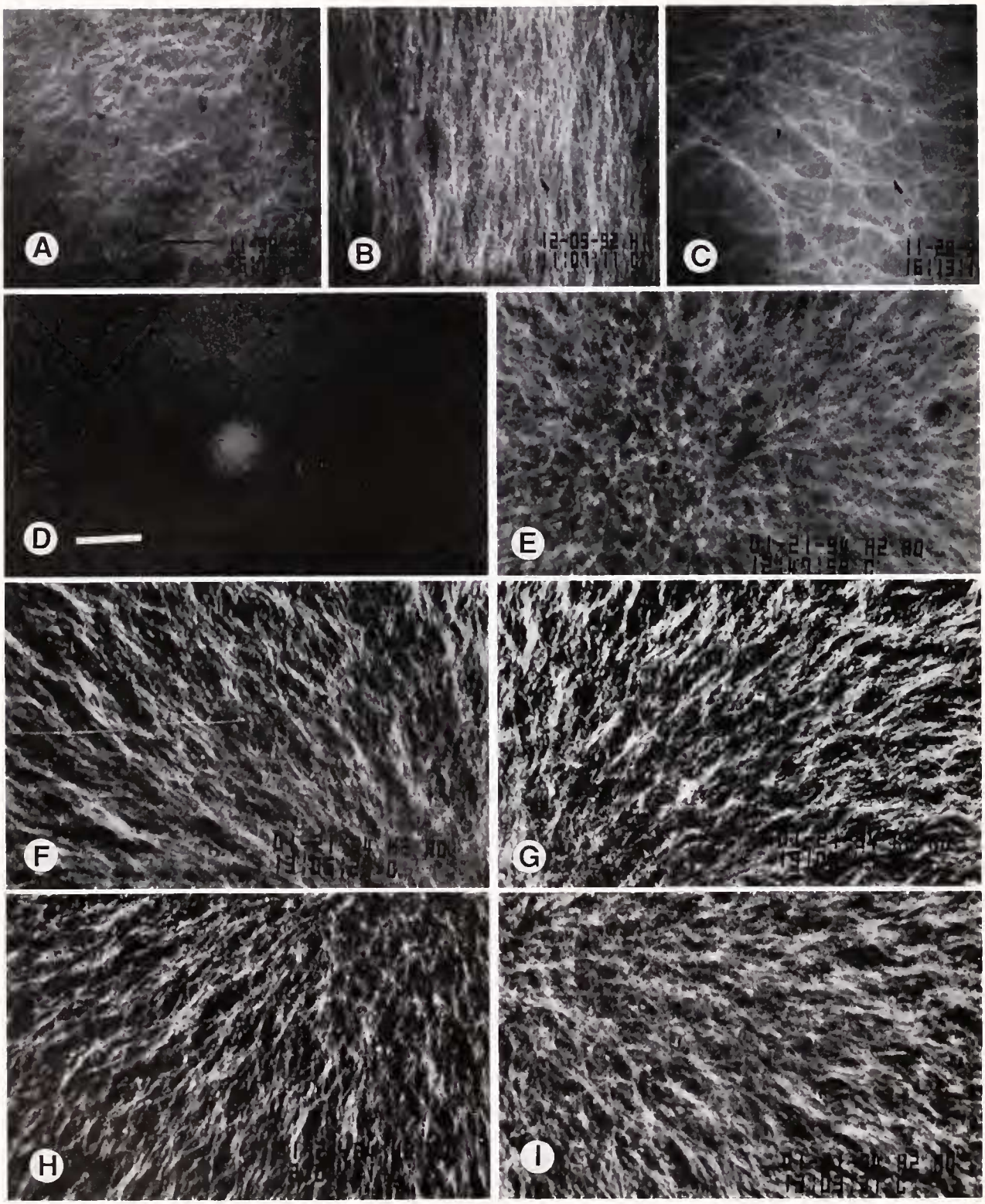

Figure 2. Microtubule arrays in eggs fixed at T_n = 0.4–1.0. All images were obtained by conventional epifluorescence microscopy. Scale bars: A, 10 μm; D, 25 μm. A–C were printed at one magnification, D–I at another. (A) Equatorial ooplasm of an egg fixed at T_n = 0.4. The animal-vegetal axis runs from lower left to upper right. The microtubule network here is denser than in eggs fixed at T_n = 0.16 (compare with Fig. 1C) and still has no apparent preferred orientation. (B) The vegetal mat of parallel microtubules in an egg fixed at T_n = 0.4. Practically all the microtubules share a single orientation in this mat, which we saw at T_n = 0.24–0.76. (C) Ooplasm at the vegetal pole of an egg fixed at T_n = 1.0. The parallel organization of microtubules near the vegetal pole is gone. (D and E) The same microscopic field of a double-stained egg

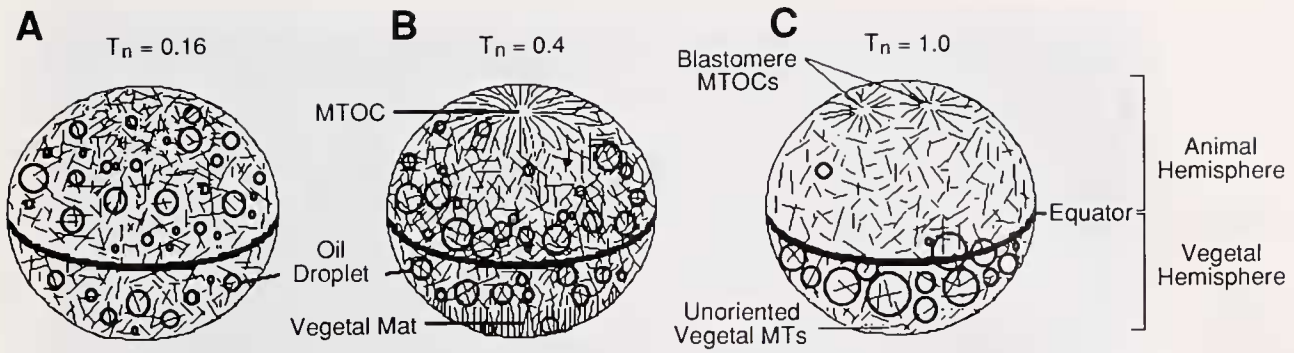

Figure 3. Summary of the spatial distribution of microtubules in medaka during the first cell cycle. The diagrams were drawn approximately to scale with respect to the size of the microtubule-organizing center, the vegetal mat, and oil droplets; but the thickness of individual microtubules has been greatly exaggerated to demonstrate the arrays clearly. The diameter of the egg is about 1140 μm. (A) Microtubules in an egg fixed at $T_n = 0.16$. An unoriented network of microtubules, denser near the animal pole, is present throughout the egg. (B) Microtubules in an egg fixed at $T_n = 0.4$. An array of microtubules that radiate from a zone in the blastodisc near the pronuclei forms by $T_n = 0.3$ and persists until at least $T_n = 0.76$, while at the vegetal pole, a mat of parallel microtubules forms by $T_n = 0.24$ and persists until at least $T_n = 0.76$. Microtubules in interpolar ooplasm have no preferred orientation at any time. Note that most of the oil droplets from the animal hemisphere have moved into the equatorial region by this time. (C) Microtubules in an egg fixed at $T_n = 1.0$. Two microtubule-organizing centers, one at each pole of the dividing blastodisc, are present. The density of microtubules in interpolar ooplasm has decreased, and the parallel organization of microtubules at the vegetal pole has been lost.

of these blastomeres had a microtubule-organizing center (data not shown) similar to the one present in the blastodisc from $T_n = 0.30$ to at least $T_n = 0.76$. The parallel organization of the microtubule network near the vegetal pole was lost by this stage (Fig. 2C). The pattern of microtubules in eggs fixed at $T_n \approx 1.0$ is summarized in Fig. 3C.

Microtubule networks in eggs injected with 5,5'-dibromo-BAPTA

The effects of injected KCl and dibromo-BAPTA on microtubule networks are summarized in Figures 4 and 5. The microtubule networks in eggs into which we injected KCl were indistinguishable from those found in uninjected eggs fixed at the same time ($T_n = 0.76$ [from 57 min to 84 min after fertilization, depending on the temperature]; Fig. 4A [compare with Fig. 2B], 5A [compare with Fig. 2A]). The parallel organization of microtubules in the vegetal mat was not disrupted by dibromo-BAPTA (Fig. 4B). However, the injection of dibromo-BAPTA had profound effects on the microtubule networks near the animal pole, where the radiating pattern of microtubules near the animal pole was disrupted (Fig. 4C, D). The only apparent effect of dibromo-BAPTA on the microtubule arrays in the equatorial region was a decrease in the density of microtubules near the injection site (Fig. 5B, C).

Dibromo-BAPTA also inhibited the movement of the pronuclei. At $T_n \approx 0.5$, the distance between the male and female pronuclei was as follows: uninjected control eggs, 1.8 ± 3.0 μm ($\bar{X} \pm$ SD, $n = 10$ eggs); eggs into which we injected KCl, 1.7 ± 3.4 μm ($n = 4$ eggs); eggs into which we injected dibromo-BAPTA, 40.4 ± 28.6 μm ($n = 5$ eggs). A one-way analysis of variance and *post-hoc* Student's *t*-tests revealed that the BAPTA-treated eggs differed significantly ($P = 0.038$) from the other two treatments.

Discussion

The pattern of microtubules in the fertilized medaka egg varied both temporally and spatially during the first cell cycle. Temporal changes included an increase in the density of microtubules throughout the ooplasm and changes in the degree of orientation of microtubules in

($T_n = 0.4$) is shown, using either a filter to show the fusing Hoechst-stained pronuclei (D) or one to show rhodamine-stained microtubules (E). Microtubules radiate from a region near the pronuclei, roughly following meridian lines. (F–I) These are photographs of four quadrants around, and just outside, the region containing the pronuclei. Note the strong orientation of microtubules along meridian lines. The pronuclei are to lower right in F, lower left in G, upper right in H, upper left in I.

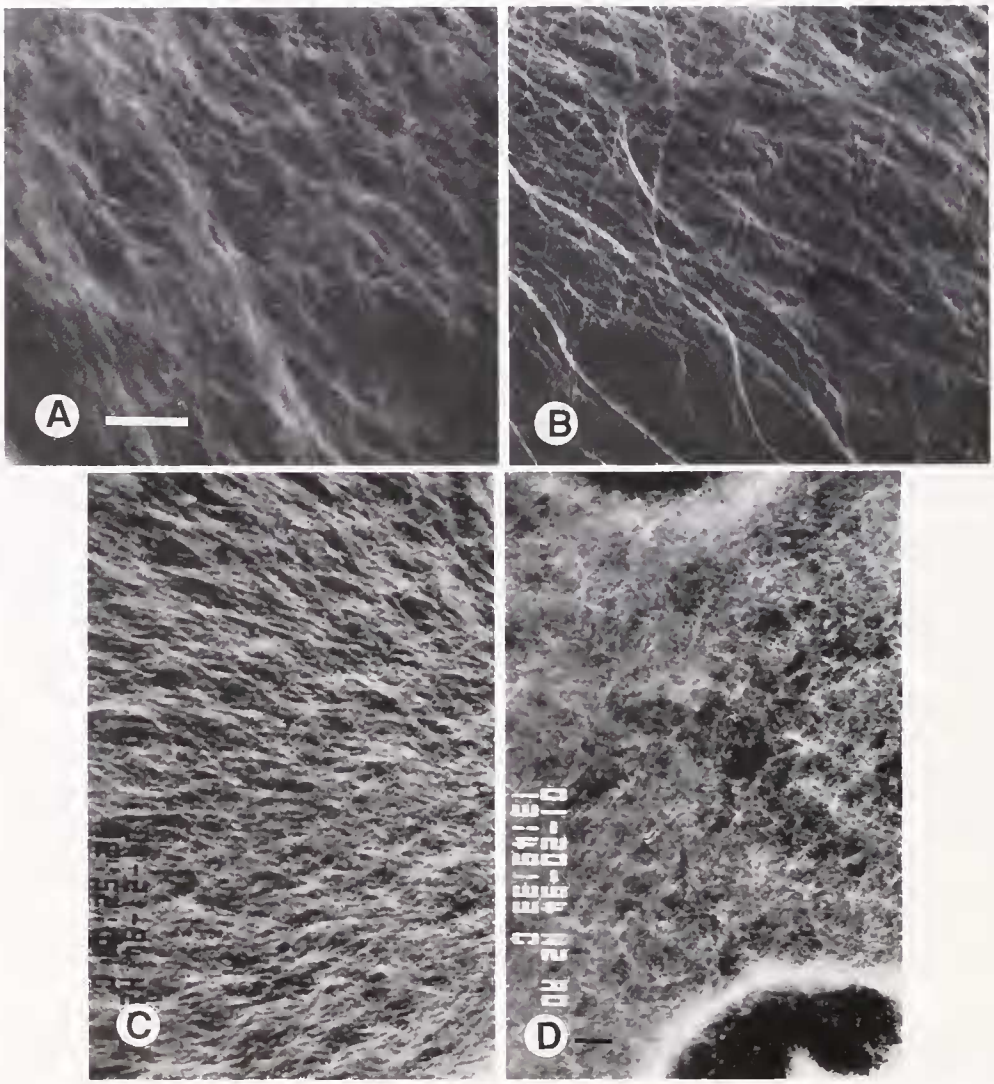

Figure 4. The effect of dibromo-BAPTA on microtubule arrays in polar ooplasm. All eggs were fixed at $T_n = 0.50$. A and B are confocal images obtained using the Zeiss laser scanning confocal microscope; C and D were obtained by standard epifluorescence microscopy. Scale bar = 10 μm; A and B are at the same magnification, C and D at another. (A and B) Injection of neither KCl (A) nor dibromo-BAPTA (B; fixed 32 min after fertilization and about 26 min after injection of dibromo-BAPTA) had any apparent effect on the parallel array of microtubules in the vegetal mat. (C) Microtubules are oriented along meridian lines near the animal pole of this control (uninjected) egg. The pronuclei are to the right of the region shown in this photograph. (D) Injection of dibromo-BAPTA disrupted the radial pattern of microtubules in the blastodisc. This egg was fixed about 52 min after fertilization and about 46 min after the injection of dibromo-BAPTA. Note the absence of radially oriented microtubules in this photograph, which is of the same region of the egg as the one shown in Fig. 4C.

the polar regions of the egg. The striking feature of the region near the animal pole was the development of an array of microtubules that radiated from near the pronuclei to approximately 30° arc from the animal pole. Though microtubules were initially ($T_n = 0.08$) present near the animal pole as a sparse unoriented network, a dense network of radially oriented microtubules had formed by $T_n = 0.3$. Such radial arrays of microtubules are present in fertilized eggs of a number of animals, including annelids (Astrow *et al.*, 1989), ctenophores (Houliston *et al.*, 1993), echinoderms (Harris *et al.*, 1980), ascidians (Sawada and Schatten, 1988), and amphibians (Houliston and Elinson, 1991; Schroeder and Gard, 1992; Elinson and Palaček, 1993), and are associated with the sperm aster and sometimes with the female pronucleus as well.

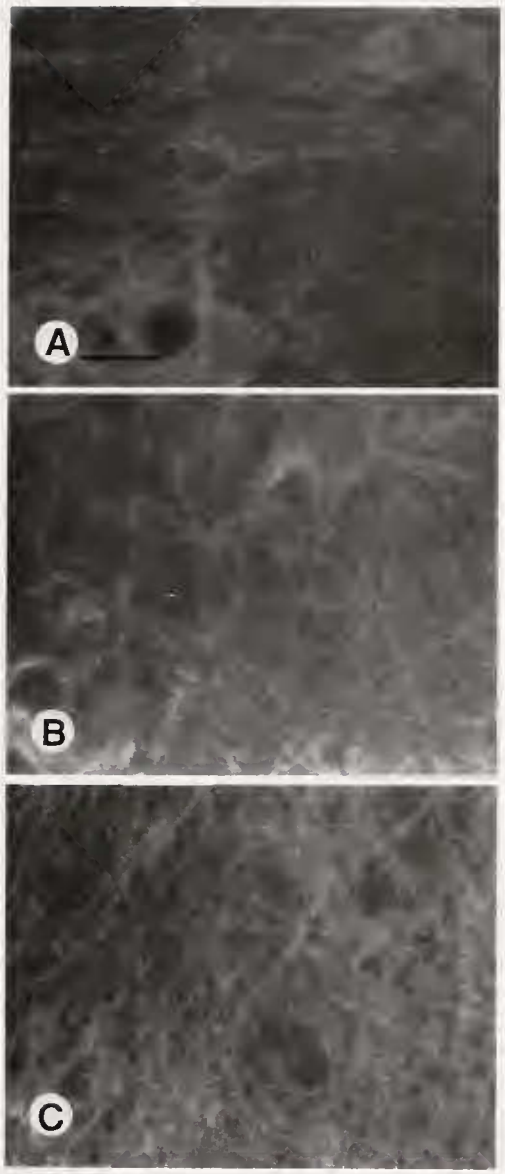

Figure 5. The effects of KCl and dibromo-BAPTA on microtubule arrays in equatorial ooplasm. All eggs were fixed at $T_n = 0.76$ (about 60 min after fertilization and about 54 min after injection of dibromo-BAPTA), and all images were obtained using the Zeiss laser scanning confocal microscope. Scale bar, 10 μm. (A) In eggs into which we injected KCl, the array of microtubules was similar to uninjected controls (not shown). The animal-vegetal axis runs from left to right. (B and C) Injection of dibromo-BAPTA appeared to decrease the density of microtubules near the injection site (B; the animal-vegetal axis runs from right to left) relative to the density observed at the antipode of the injection site (C; the animal-vegetal axis runs from bottom to top).

The mat of parallel microtubules at the vegetal pole of the medaka egg is reminiscent of the one found at the vegetal pole of amphibian eggs, where it is involved in the cortical rotation that forms the gray crescent and thus determines the dorsal-ventral axis of the embryo (Manes *et al.*, 1978; Scharf and Gerhart, 1983; Vincent *et al.*, 1987; Gerhart *et al.*, 1989; Elinson and Rowning, 1988; Elinson and Palaček, 1993). A similar array of parallel microtubules is also present at the vegetal pole of the zebrafish (*Danio rerio*) egg (see Fig. 9C in Strähle and Jesuthasan, 1993). Although there is no evidence for the occurrence of a cortical rotation in the medaka egg, embryos of some primitive fishes that undergo holoblastic cleavage (species in the Superorder Chondrostei within the Actinopterygii, for example the sturgeon, *Acipenser güldenstädti*) do form a gray crescent and thus perhaps do undergo a cortical rotation (reviewed by Bolker, 1993; see also Clavert, 1962; Ginsburg and Dettlaff, 1991). In amphibian eggs, the plane of the first cleavage is parallel to the microtubules near the vegetal pole; and in both amphibians and primitive fishes, the plane of the first cleavage bisects the gray crescent along a meridian (Bolker, 1993). We are currently pursuing the question of the relationship between the orientation of microtubules in the vegetal mat and that of the embryonic axes in the medaka egg. In both *Xenopus laevis* and the medaka, the parallel orientation of the microtubules in the vegetal pole region is transient. In *X. laevis*, this mat begins to form at $T_n \approx 0.55$ and disappears after $T_n \approx 0.8$ (Elinson and Palacek, 1993). In medaka eggs, it is present by $T_n \approx 0.24$ and is still present at $T_n \approx 0.76$; but by the beginning of the first cleavage, the network has lost its parallel organization.

In sharp contrast to the strongly oriented networks of microtubules in polar ooplasm, interpolar ooplasm contained a network of crisscrossed microtubules having no apparent preferred orientation. Microtubules were present here by $T_n = 0.08$ and subsequently increased in density through $T_n = 0.24$. The lack of orientation of microtubules in this region of the medaka eggs contrasts with the situation in the zebrafish egg, in which microtubules are oriented along the animal-vegetal axis during both the first cell cycle and epiboly (Strähle and Jesuthasan, 1993; Solnica-Krezel and Driever, 1994).

Because microtubule poisons inhibit the movement of oil droplets toward the vegetal pole of the medaka egg, it has been suggested that these droplets are transported along microtubules by microtubule-based motors (Abraham *et al.*, 1993a). Further, because oil droplets move toward the vegetal pole roughly along meridians, we predicted that a network of microtubules, also oriented more or less along meridians, would extend from the animal pole to near the vegetal pole. Although such a pattern did develop near the animal pole by $T_n = 0.3$, a time when oil droplets have begun to move toward the vegetal pole, we saw no such preferred orientation of microtubules in most of the interpolar ooplasm, suggesting that oil droplets move toward the vegetal pole along a biochemically dis-

tinct (Gard, 1991; Wolff *et al.*, 1992) subset of interpolar microtubules that are oriented along meridian lines.

The movement of most oil droplets toward the vegetal pole of the medaka egg begins at $T_n \approx 0.15$–0.30 (Catalone and Fluck, 1994). The results of the present study, which show that microtubules are present before oil droplets begin to move toward the vegetal pole, suggest that this movement is triggered by some factor other than the appearance of microtubules. We have also shown that even though the movement of oil droplets is "frozen" at the antipode of the site at which dibromo-BAPTA is injected into the egg (Fluck *et al.*, 1994), many microtubules are present in this region of the ooplasm. Factors that could initiate the movement of oil droplets toward the vegetal pole include the formation of an appropriate subtype of microtubules, the activation of a microtubule-based motor such as kinesin (Brady *et al.*, 1990; Schnapp *et al.*, 1992), fulfillment of a requirement that a minimum number of microtubules be associated with an oil droplet before it begins to move, or a gel-sol transition of the ooplasm (Janson and Taylor, 1993) that frees the droplets and enables them to move toward the vegetal pole.

We have also demonstrated in the present study that injection of dibromo-BAPTA into medaka eggs affects the pattern of microtubules in the egg. This relatively weak calcium buffer ($K_D = 1.5\ \mu M$; Pethig *et al.*, 1989) is believed to act as a shuttle buffer, one that binds Ca^{2+} at the high end of a $[Ca^{2+}]$ gradient and releases it at the low end; in other words, the buffer facilitates the diffusion of Ca^{2+} within the cell (Speksnijder *et al.*, 1989). The time between injection of dibromo-BAPTA and fixation of the eggs in the present study was sufficient for the buffer to diffuse to both the animal pole and vegetal pole, to dissipate cytosolic Ca^{2+} gradients near the poles, and to inhibit the formation of the blastodisc and the movement of oil droplets toward the vegetal pole (Fluck *et al.*, 1992, 1994).

Our results suggest that at least some of the effects of dibromo-BAPTA on ooplasmic segregation in the medaka egg are caused by its disruption of microtubule formation and organization, which are controlled by a number of calcium-binding regulatory proteins (Weisenberg, 1972; Schliwa *et al.*, 1981; Keith *et al.*, 1983; Lieuvin *et al.*, 1994). Facilitated diffusion theory predicts that calcium buffer concentrations similar to those found effective in the present study act by dissipating zones of cytosolic $[Ca^{2+}]_{free}$ in the micromolar range (Speksnijder *et al.*, 1989). An example of a protein that is responsive to changes in $[Ca^{2+}]_{free}$ in this range is calmodulin (Cheung, 1980), which regulates the activity of proteins that interact with microtubules (Ishikawa *et al.*, 1992).

The inhibition of pronuclear movements by dibromo-BAPTA is consistent with the explanation that the buffer disrupts the organization of microtubules near the animal pole. In a number of species, including the medaka, the movement of the pronuclei is inhibited by microtubule poisons (Hiramoto *et al.*, 1984; Sawada and Schatten, 1989; Abraham *et al.*, 1993a), suggesting that microtubules are necessary for these movements.

The parallel array of microtubules near the vegetal pole was apparently resistant to the effects of the buffer, suggesting that microtubules in this region of the egg differ in some way from those in other regions of the egg. This possible difference could be probed by microinjecting a microtubule poison, for example demecolcine, directly into the vegetal ooplasm.

The suggestion that the medaka egg has two independent microtubule networks is consistent with the situation in *X. laevis*, in which two independent networks of microtubules are present during the first cell cycle: one is near the animal pole and is associated with the pronuclei, while the other is the parallel array of microtubules near the vegetal pole (Elinson and Rowning, 1988; Houliston and Elinson, 1991; Elinson and Palaček, 1993; Sardet *et al.*, 1994). Moreover, in both amphibian eggs (Houliston and Elinson, 1991; Elinson and Palaček, 1993) and medaka eggs (Webb and Fluck, unpub. obs.), vegetal cortical arrays of microtubules form in parthenogenetically activated eggs. Using the "Colcemid-UV" method (Hiramoto *et al.*, 1984; Webb and Fluck, 1993), we are currently pursuing the question of the existence of independent arrays of microtubules in the animal pole region, vegetal pole region, and interpolar ooplasm. Our data at this time do not permit us to say whether microtubules are continuous from one region of the egg to another.

Acknowledgments

Supported by NSF DCB-9017210 and NSF MCB-9316125 to RAF, NSF BIR 9211855 to Lionel F. Jaffe and ALM, and grants from Franklin & Marshall College's Hackman Scholar Program and Harry W. and Mary B. Huffnagle Fund to VCA. Louis Kerr provided technical assistance in the use of the laser scanning confocal microscope in the Central Microscope Facility at the Marine Biological Laboratory, Tamika Webb assisted in the preparation and examination of one batch of eggs, and Bob Golder assisted in the preparation of Figure 3. The research at Carnegie-Mellon University was supported by National Science Foundation and Technology Center grant DIR-8920118. We thank Robbin L. DeBiasio for image acquisition, data processing, and 3-D representation; and Gregory M. LaRocca for technical assistance and image acquisition.

Literature Cited

Abraham, V. C., S. Gupta, and R. A. Fluck. 1993a. Ooplasmic segregation in the medaka (*Oryzias latipes*) egg. *Biol. Bull.* **184:** 115–124.

Abraham, V. C., A. L. Miller, L. F. Jaffe, and R. A. Fluck. 1993b. Cytoplasmic microtubule arrays in *Oryzias latipes* (medaka) eggs during ooplasmic segregation. *Biol. Bull.* **185:** 305–306.

Astrow, S. H., B. Holton, and D. A. Donovan. 1989. Teloplasm formation in a leech, *Helobdella triserialis*, is a microtubule-dependent process. *Dev. Biol.* **135:** 306–319.

Beams, H. W., R. G. Kessel, C. Y. Shih, and H. N. Tung. 1985. Scanning electron microscopy studies on blastodisc formation in the zebrafish, *Brachydanio rerio*. *J. Morphol.* **184:** 41–49.

Bolker, J. A. 1993. Gastrulation and mesoderm morphogenesis in the white sturgeon. *J. Exp. Zool.* **266:** 116–131.

Brady, S. T., K. K. Pfister, and G. S. Bloom. 1990. A monoclonal antibody against kinesin inhibits both anterograde and retrograde fast axonal transport in squid axoplasm. *Proc. Natl. Acad. Sci. USA* **87:** 1061–1065.

Catalone, B. J., and R. A. Fluck. 1994. Oil droplet movement during ooplasmic segregation in the medaka fish egg (*Oryzias latipes*). *J. PA Acad. Sci.* **67:** 173.

Cheung, W. Y. 1980. Calmodulin—an introduction. Pp. 1–12 in *Calmodulin and Cell Function*, Vol. 1, W. Y. Cheung, ed. Academic Press, Orlando, FL.

Clavert, J. 1962. Symmetrization of the egg of vertebrates. Pp. 27–60 in *Advances in Morphogenesis*, Vol. 2, M. Abercrombie and J. Brachet, eds. Academic Press, New York.

Elinson, R. P., and J. Palaček. 1993. Independence of two microtubular systems in fertilized frog eggs: the sperm aster and the vegetal array. *Roux's Arch. Dev. Biol.* **202:** 224–232.

Elinson, R. P., and B. Rowning. 1988. A transient array of parallel microtubules in frog eggs: potential tracks for a cytoplasmic rotation that specifies the dorso-ventral axis. *Dev. Biol.* **128:** 185–197.

Fluck, R. A., A. L. Miller, and L. F. Jaffe. 1992. High calcium zones at the poles of developing medaka eggs. *Biol. Bull.* **183:** 70–77.

Fluck, R. A., A. L. Miller, V. C. Abraham, and L. F. Jaffe. 1994. Calcium buffer injections inhibit ooplasmic segregation in medaka eggs. *Biol. Bull.* **186:** 254–262.

Gard, D. L. 1991. Organization, nucleation, and acetylation of microtubules in *Xenopus laevis* oocytes: a study by confocal immunofluorescence microscopy. *Dev. Biol.* **143:** 346–362.

Gerhart, J., M. Danilchik, T. Doniach, S. Roberts, B. Rowning, and R. Stewart. 1989. Cortical rotation of the *Xenopus* egg: consequences for the anteroposterior pattern of embryonic dorsal development. *Development* **1989 Supplement:** 37–51.

Ginsburg, A. S., and T. A. Dettlaff. 1991. The Russian sturgeon *Acipenser güldenstädti*. Part 1. Gametes and early development up to time of hatching. Pp. 15–65 in *Animal Species for Developmental Studies*, Vol. 2, *Vertebrates*. T. A. Dettlaff and S. G. Vassetsky, eds. Consultants Bureau, New York.

Harris, P., M. Osborn, and K. Weber. 1980. Distribution of tubulin-containing structures in the egg of the sea urchin *Strongylocentrotus purpuratus* from fertilization through first cleavage. *J. Cell Biol.* **84:** 668–679.

Hiramoto, Y., M. S. Hamaguchi, Y. Nakano, and Y. Shoji. 1984. Colcemid uv-microirradiation method for analyzing the role of microtubules in pronuclear migration and chromosome movement in sand-dollar eggs. *Zool. Sci.* **1:** 29–34.

Houliston, E., D. Carré, J. A. Johnston, and C. Sardet. 1993. Axis establishment and microtubule-mediated waves prior to first cleavage in *Beroe ovata*. *Development* **117:** 75–87.

Houliston, E., and R. P. Elinson. 1991. Patterns of microtubule polymerization relating to cortical rotation in *Xenopus laevis* eggs. *Development* **112:** 107–117.

Inoué, S. 1981. Video image processing greatly enhances contrast, quality, and speed in polarization-based microscopy. *J. Cell Biol.* **89:** 346–356.

Ishikawa, R., O. Kagami, C. Hayashi, and K. Kohama. 1992. Characterization of smooth muscle caldesmon as a microtubule-associated protein. *Cell Motil. Cytoskel.* **23:** 244–251.

Janson, L. W., and D. L. Taylor. 1993. *In vitro* models of tail contraction and cytoplasmic streaming in amoeboid cells. *J. Cell Biol.* **123:** 345–356.

Keith, C., M. DiPaola, F. R. Maxfield, and M. L. Shelanski. 1983. Microinjection of Ca^{++}-calmodulin causes a localized depolymerization of microtubules. *J. Cell Biol.* **97:** 1918–1924.

Lieuvin, A., J.-C. Labbé, M. Dorée, and D. Job. 1994. Intrinsic microtubule stability in interphase cells. *J. Cell Biol.* **124:** 985–996.

Manes, M. E., R. P. Elinson, and F. D. Barbieri. 1978. Formation of the amphibian grey crescent: effects of colchicine and cytochalasin B. *Roux's Arch. Dev. Biol.* **185:** 99–104.

Pethig, R., M. Kuhn, R. Payne, E. Adler, T.-H. Chen, and L. F. Jaffe. 1989. On the dissociation constants of BAPTA-type calcium buffers. *Cell Calcium* **10:** 491–498.

Sardet, C., A. McDougall, and E. Houliston. 1994. Cytoplasmic domains in eggs. *Trends Cell Biol.* **4:** 166–172.

Sawada, T., and G. Schatten. 1988. Microtubules in ascidian eggs during meiosis, fertilization, and mitosis. *Cell Motil. Cytoskel.* **9:** 219–230.

Sawada, T., and G. Schatten. 1989. Effects of cytoskeletal inhibitors on ooplasmic segregation and microtubule organization during fertilization and early development in the ascidian *Molgula occidentalis*. *Dev. Biol.* **132:** 331–342.

Scharf, S. R., and J. C. Gerhart. 1983. Axis determination in eggs of *Xenopus laevis*: a critical period before first cleavage, identified by the common effects of cold, pressure, and ultraviolet irradiation. *Dev. Biol.* **99:** 75–87.

Schliwa, M., U. Euteneuer, J. C. Bulinski, and J. G. Izant. 1981. Calcium lability of cytoplasmic microtubules and its modulation by microtubule-associated proteins. *Proc. Natl. Acad. Sci. USA* **78:** 1037–1041.

Schroeder, M. M., and D. L. Gard. 1992. Organization and regulation of cortical microtubules during the first cell cycle of *Xenopus* eggs. *Development* **114:** 699–709.

Schnapp, B. J., T. S. Reese, and R. Bechtold. 1992. Kinesin is bound with high affinity to squid axon organelles that move to the plus-end of microtubules. *J. Cell Biol.* **119:** 389–399.

Solnica-Krezel, L., and W. Driever. 1994. Microtubule arrays of the zebrafish yolk cell: organization and function during epiboly. *Development* **120:** 2443–2455.

Speksnijder, J. E., A. L. Miller, M. H. Weisenseel, T.-H. Chen, and L. F. Jaffe. 1989. Calcium buffer injections block fucoid egg development by facilitating calcium diffusion. *Proc. Natl. Acad. Sci. USA* **86:** 6607–6611.

Strähle, U., and S. Jesuthasan. 1993. Ultraviolet irradiation impairs epiboly in zebrafish embryos: evidence for a microtubule-dependent mechanism of epiboly. *Development* **119:** 909–919.

Vincent, J.-P., S. R. Scharf, and J. C. Gerhart. 1987. Subcortical rotation in *Xenopus* eggs: a preliminary study of its mechanochemical basis. *Cell Motil. Cytoskel.* **8:** 143–154.

Webb, T. A., and R. A. Fluck. 1993. Microfilament- and microtubule-based movements during ooplasmic segregation in the medaka fish egg (*Oryzias latipes*). *Mol. Biol. Cell* **4:** 274a.

Weisenberg, R. C. 1972. Microtubule formation *in vitro* in solutions containing low calcium concentrations. *Science* **177:** 1104–1105.

Wolff, A., B. Néchaud, D. Chillet, H. Mazarguil, E. Desbruyères, S. Audebert, B. Eddé, F. Gros, and P. Denoulet. 1992. Distribution of glutamylated α and β-tubulin in mouse tissues using a specific monoclonal antibody, GT335. *Eur. J. Cell Biol.* **59:** 425–432.